The correct citation for the paper is:

Rees, S.J. and P. Haves. 1999. A Nodal Model for Displacement Ventilation and Chilled Ceiling Systems, *Proc. of 'Building Simulation-99'*, Kyoto, Japan, September 13-15, 1:433-440.

A NODAL MODEL FOR DISPLACEMENT VENTILATION AND CHILLED CEILING SYSTEMS IN OFFICE SPACES

Simon J. Rees[†] and Philip Haves[‡]

[†]School of Mechanical & Aerospace Engineering,
Oklahoma State University, Stillwater, OK 74074, USA.
[‡]Lawrence Berkeley National Laboratory, 1 Cyclotron Road, MS 90-3111,
Berkley, CA 94720, USA.

ABSTRACT

A nodal model has been developed to represent room heat transfer in displacement ventilation and chilled ceiling systems. The model uses precalculated air flow rates to predict the air temperature distribution and the division of the cooling load between the ventilation air and the chilled ceiling. The air movements in the plumes and the rest of the room are represented separately using a network of ten air nodes. The values of the capacity rate parameters are calculated by solving the heat and mass balance equations for each node using measured temperatures as inputs. Correlations between parameter values for a range of cooling loads and supply air flow rates are presented.

INTRODUCTION

Displacement ventilation and chilled ceilings and are complementary ventilation and cooling technologies that have the potential to provide better comfort, air quality and energy consumption than conventional systems. Displacement ventilation used with or without a chilled ceiling is characterized by distinct vertical temperature gradients and radiant asymmetry. These characteristics prevent such systems being simulated by current annual energy simulation programs, in which it is assumed that room air is well mixed and surfaces are isothermal.

In office displacement ventilation systems, air is introduced at the diffuser at a temperature slightly below the mean air temperature in the space and flows across the floor before being transported vertically by the plumes associated with heat sources in the room (see Figure 1). This generally upward movement of air results in a warm layer of mixed air adjacent to the ceiling, resulting in a positive temperature gradient over most of the height of the room.

Thermal comfort considerations impose an upper limit to the allowable vertical temperature gradients in office spaces of 2-3 K/m. Since these gradients are largely a function of internal load and room height, this results in a practical cooling load limit for these systems of about 30-40W/m^2. It is for this reason that, in many applications, displacement ventilation is used with a chilled ceiling. By using the ceiling as an additional source of convective and radiant cooling, the capacity of such systems may be increased to approximately 80W/m^2. Chilled ceilings are also complementary to displacement ventilation systems, in that they can operate with similar primary chilled water temperatures. This chilled water temperature can be significantly higher than in conventional cooling systems (~15^{o}C *vs.* ~6 ^{o}C) if dehumidification is not required or can be achieved in some other way, e.g. by the use of desiccants. Depending on the climate, it may be possible to use evaporative cooling on both the air side and the water side and eliminate the use of refrigeration systems.

A model has been developed that is able to capture the effects of the vertical air and surface temperature gradients of these systems and is computationally efficient enough for annual energy simulation. The model has a network of ten air nodes that are used to represent the room bulk air flow. The walls are subdivided to treat vertical variations in surface temperature and heat flux. The paper describes the development of the structure of the nodal network used in the model.

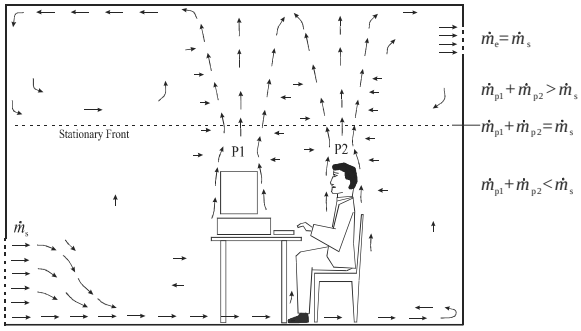

Figure 1: Flow in a typical office displacement ventilation system.

The principal parameters of this type of model of the convection coefficients and air capacity rates. Some nodal models (Dalicieux and Bouia 1993) perform momentum-pressure balances at the room air nodes using a reduced form of the Navier-Stokes equations. This is not done here, however, so the capacity rates between interconnected air nodes are parameters of the model that have to be predetermined. In the model proposed here, there are ten air nodes, requiring the definition of four independent capacity rates. The capacity rate parameters of the model can be

calculated by solving the heat and mass balance equations of the nodal model using measured temperatures as inputs. The variation of the model parameters with both design parameters and operating conditions is analyzed and simple rules for predicting the model parameters are derived. This approach could also be used to find the parameters of nodal models of other systems where intra-zone airflow is modeled explicitly.

A generalized nodal thermal modeling program LIGHTS (Sowell 1989) was used as a prototyping tool to develop the model presented here. The model could be implemented in a modular simulation program, as described in Rees and Haves (1995) or as an extension of the room model in a whole building energy simulation program.

The experimental data used here comes from two series of test chamber experiments. The first source of data is the displacement ventilation experiments conducted at the National Swedish Institute for Building Research by Li *et al.* (1993). The authors also made measurements in a test chamber at Loughborough University (Rees 1998). This test chamber had a single displacement ventilation diffuser and a flat panel chilled ceiling occupying 88% of the ceiling area. Air temperature measurements were made using eighteen shielded thermocouples. Approximately 50 thermocouples were used to make surface temperature measurements.

THE MODEL STRUCTURE

The following considerations guided the development of the structure of the model:

- the quantities that the model is required to predict;
- the degree of detail required adequately to represent the heat transfer phenomena of interest;
- the bulk air flow movements observed in the experiments and predicted by CFD.

The first two considerations influenced the complexity of the model. The third was used to determine the topology of the nodal network.

The structure of a nodal model of a displacement ventilation and chilled ceiling system has to be more complex than that of a conventional fully mixed system because, firstly, the output requirements are different, and, secondly, the assumption of isothermal surfaces is no longer valid. One of the output requirements is the room operating/comfort temperature. This temperature lies somewhere between the air temperature adjacent to the floor and the extract temperature, and is conventionally measured at a height of 1.1m. This imposes a requirement either to place a node at that height, or to interpolate between nodes above and below. The other basic output requirements of the model are the air and water stream heat flows, and so inlet and outlet air and water stream nodes are also required.

Given this minimal set of nodes necessary to provide the required output, further nodes are required to capture air and surface temperature gradients. The walls are divided vertically into four equal sections, requiring a surface node and adjacent air node at each level. The presence of buoyancy-dominated boundary layers flowing over the floor and ceiling suggests that separate floor and ceiling air nodes are required.

Other nodal models of displacement ventilation (Mundt 1990, Li *et al.* 1993, Hensen and Huygen 1996) have had room air nodes connected in a serial fashion. Models with this one-dimensional 'plug flow' arrangement make reasonable predictions of the air temperature just above the floor and just below the ceiling but significantly over-predict the room air and wall temperatures (Rees and Haves, 1995). The excessive air temperatures predicted in the lower part of the room are a consequence of the room air nodes having a direct connection with the heat load. In rooms with displacement ventilation, there is some de-coupling of the heat loads from the room air (the air surrounding the plumes, that is) by virtue of the heat being transported to high level directly by the plumes.

In order to account for this de-coupling effect, a second set of air nodes is introduced to represent conditions in the plume(s) explicitly. These plume air nodes are connected to each other and to the room air nodes. Vertical connections are introduced between adjacent plume nodes to represent air flow in the plume(s) and lateral connections are introduced between the room air nodes and the adjacent plume air nodes to represent entrainment of air into the plume from the surrounding air. This model structure is shown in Figure 2. The upper zone of the room is treated as being well mixed, on the assumption that the 'stationary front' would be approximately three-quarters of the way up the room.

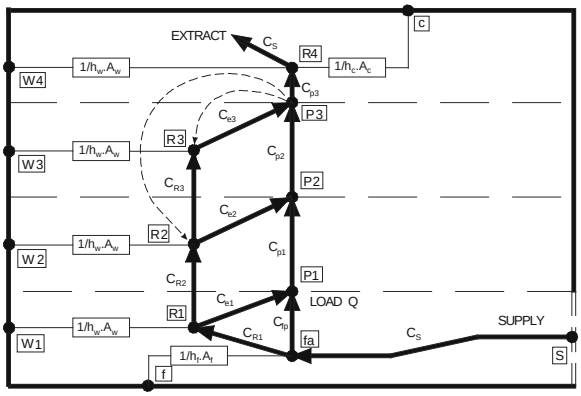

Figure 2: A prototype nodal model of a room with displacement ventilation showing separate plume and room air nodes (as in Rees and Haves 1995).

Results for this form of the nodal model are shown in Figure 3. These results show good agreement of the air temperatures at the first two nodes and near the ceiling but otherwise too small a temperature gradient in the lower and middle parts of the room. The experimental data, however, generally show the steepest air temperature gradients to be in the lower part of the room. This can not be accounted for if the direction of the flow in the air surrounding the plume (i.e. between nodes R1 and R2, R2 and R3 in Figure 2) is always upwards. This is because the only temperature gains with increasing height are due to the convective fluxes at each level. The convective fluxes predicted assuming reasonable values of the convection coefficients are insufficient to produce temperature gradients of the magnitude recorded experimentally.

It would seem that the only mechanism that can account for sufficient heat being transferred to the middle and lower part of the room, is bulk movement of air from the warm layer near the ceiling to lower in the room i.e. by a significant amount of recirculation.

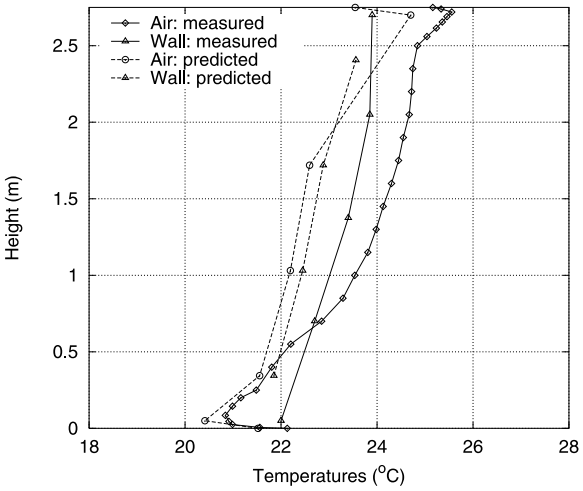

Figure 3: Air and wall temperature profiles predicted by the nodal model shown in Figure 2 (Li *et al.* Case B3).

It is not obvious which path between air nodes in the model corresponds to the recirculation of air from the upper to lower parts of the room. In previous work (Rees and Haves 1995, Haves *et al.* 1995) recirculation was simply introduced in the model structure by making two connections from the room air node in the upper zone to the air nodes in the middle zones. This arrangement is shown by the dotted lines from node P3 in Figure 2. The correct temperature gradients and coupling with the walls is reproduced for this data set by assuming 60%.

Definitive determination of the structure of the air flow network ideally requires experimental measurement of the flow field for the whole room. Laser Doppler anemometry would be required, which is both time-consuming and expensive. An alternative approach is to use the results of computational fluid dynamics (CFD) simulations to help refine the air flow network in the nodal model and this approach has been used here.

The velocity field data generated using CFD (Rees 1998) have been aggregated by dividing the room up with hypothetical surfaces to form a number of large control volumes. These large control volumes have been arranged so that the flow through each surface is at a position representative of the flow into and out of the plume or between each horizontal layer. The numerical velocity data were then integrated over the faces of these large control volumes to find the net mass fluxes. These flows are presented in two-dimensional form in Figure 4 for one particular test case (DV9). It can be seen that there is strong recirculation from the upper layer to the two middle layers. The magnitude of this recirculating flow rate is large compared to the supply and extract flow rates.

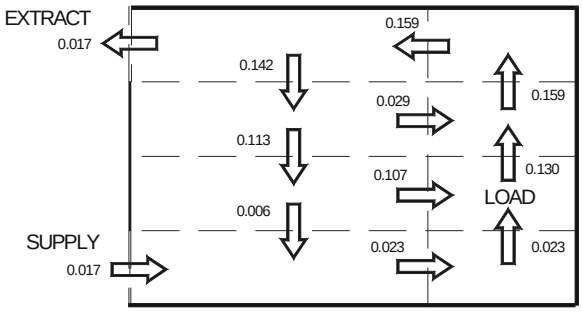

Figure 4: Bulk air flows calculated from a CFD simulation of test case DV9. The units are $kW.K^{-1}$.

A modified air flow network conforming to the flow pattern suggested by the numerical results was used subsequently to derive the parameter values. The structure of this model is shown in Figure 5.

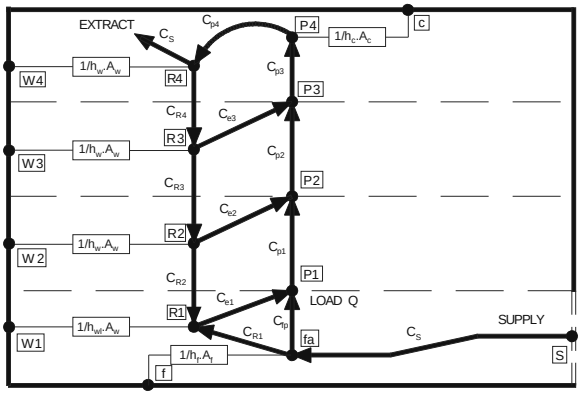

Figure 5: The model with a nodal network conforming to the air flow pattern indicated by the CFD results shown in Figure 4 (referred to as model A).

THE MODEL PARAMETERS

In a nodal model, there are heat balance and mass balance equations associated with each node. Use of the model to predict room temperature distributions requires knowledge of the capacity rates and convective heat transfer coefficients that form the parameters of these equations. The other parameters of the model are the emissivities of each room surface, the selection of which is relatively straightforward and is not discussed further.

The model structure described in the previous section and shown in Figure 5 has a total of ten air nodes, including the supply node, and the air flow network includes twelve capacity rate interconnections and six surface conductances, defined by the corresponding convective heat transfer coefficient. The capacity rates and heat transfer coefficients for each test case are calculated by simultaneously solving the inverted node air heat and mass balance equations using the corresponding set of measured air and surface temperatures.

The first step in determining the values of the parameters is to interpolate between the experimental temperature measurements to define equivalent temperature values at the air and surface nodes. The wall node temperatures, W1-W4, were obtained by interpolating between the measurements taken at different heights and producing area-weighted averages of measurements in different horizontal positions. The floor and ceiling node temperatures were obtained by taking the area-weighted averages of the measurements on these surfaces.

Measurements of the variation of air temperature with height were made using a vertical array of sensors positioned near the center of the room. Measurements at different horizontal locations outside the plumes showed very little lateral variation in air temperature, as did the CFD results.

Calculating the Parameter Values

The air node heat balance and mass balance equations were solved using a general-purpose equation solver code (Klien and Alvarado 1997). The heat transfer coefficients are inherently positive. In addition, some of the air flow rate directions are constrained in order to avoid violating the second law of thermodynamics. Experimental errors or errors in the model structure may result in the solution violating these constraints. In the chilled ceiling cases, it was found that the measured value of T_{cla} was inconsistent with positive values of both h_c and h_w. As there is more independent information pertaining to wall convection coefficients, it was decided to specify a value for h_w and calculate h_c and T_{cla}. Using the value for convective heat transfer at vertical internal surfaces suggested in the CIBSE Design Guide A (1986: Table A3.6), i.e. 3 $W.m^{-2}.K^{-1}$, yields reasonable values of ceiling coefficient for many of the test cases. The results of the parameter calculations are shown in Table 1 for the Li *et al.* test cases. The results of the calculations using the Loughborough test data are shown in Tables 2 and 3. Further details are presented in Rees (1998).

In the Li *et al.* test cases, the flow between the room air nodes R1-R4 was found to be in a downward direction so that air was recirculated from R4 down towards R1, as shown in Figure 5. In the Loughborough cases, the flow between R1 and R2 was found to be upward and the flow between R2 and R3 was sometimes upwards and sometimes downwards, although it was always quite small. This difference can be understood in terms of the positions of the heat loads in the two sets of experiments. In the Li *et al.* test cases, the load was near the floor, whereas, in the Loughborough cases, the load(s) were at desktop level. A variation of the model was introduced to deal with the latter cases, denoted 'Model B' and is shown in Figure 6.

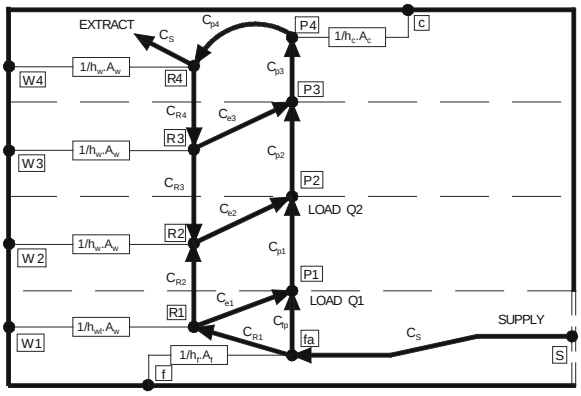

Figure 6: A variation of the model devised to conform to the results of the test chamber experiments with loads at desktop level (denoted 'Model B').

Table 1: Capacity rate and convection coefficients calculated for the Li *et al.* displacement ventilation cases. The units are W/K and $W/m^2.K$ respectively.

Case	B1	B2	B3
Load(W)	100	200	300
h_{wl}	0.89	0.92	1.3
h_w	5.5	5.5	6.3
h_c	13.91	9.88	8.51
h_f	8.60	7.25	6.06
C_S	13.86	27.7	41.6
C_{fp}	8.88	17.4	17.8
C_{e1}	9.4	15.0	26.6
C_{e2}	63.0	58.5	33.7
C_{e3}	44.7	48.2	92.4
C_{R1}/C_S	0.36	0.37	0.57
C_{e1}/C_{e2}	0.15	0.26	0.79
$C_{e1}+C_{e2}$	72.4	73.5	60.3

Table 2: Capacity rate and convection coefficients calculated for the Loughborough displacement ventilation test cases. The units are W/K and W/m^2.K respectively.

Case	DV7	DV8	DV9	DV10	DV11	DV12
Load (W)	100	200	300	300	400	400
h_{wl}	0.65	0.9	0.75	1.7	2.4	1.4
h_w	3.5	3.0	1.2	2.9	5.0	3.0
h_c	11.66	6.097	11.91	30.53	56.67	8.3
h_f	0.8	1.1	1.3	1.6	2.3	2.3
C_S	23.3	23.3	23.3	46.6	46.6	46.6
C_{fp}	6.3	6.7	2.069	9.172	1.211	9.2
C_{e1}	12.6	12.6	5.334	1.41	0.969	20.6
C_{e2}	10.33	4.8	17.6	44.03	47.81	17.3
C_{e3}	4.52	9.9	1.065	3.062	3.9	30.6
C_{R3}	5.87	0.65	1.69	7.98	3.36	0.48
C_{R1}/C_S	0.73	0.71	0.91	0.8	0.97	0.8
C_{e1}/C_{e2}	1.22	2.64	0.30	0.03	0.02	1.19
$C_{e1}+ C_{e2}$	22.93	17.30	22.93	45.44	48.78	37.91

Table 3: Capacity rate and convection coefficients calculated for the Loughborough displacement ventilation & chilled ceiling test cases. The units are W/K and W/m^2.K respectively.

Case	DC10	DC11	DC12	DC13	DC14	DC15	DC16
Load(W)	1200	800	450	450	600	600	600
T_{sw}	16	16	17	14	14	17	17
h_{wl}	0.8	1.3	0.7	1.2	1.1	1.4	1.2
h_w	3.0	3.0	3.0	3.0	3.0	3.0	3.0
h_c	4.4	5.5	6.8	4.8	6.1	6.7	6.8
h_f	5.8	2.4	1.3	1.0	2.5	3.0	2.6
C_S	46.6	46.6	46.6	46.6	46.6	46.6	23.3
C_{fp}	9.0	1.35	8.36	4.6	8.57	7.4	2.3
C_{e1}	32.7	21.83	4.95	1.0	5.37	20.1	0.9
C_{e2}	15.1	26.16	34.57	48.3	34.59	23.6	24.9
C_{e3}	303.9	11.70	18.12	120.8	46.05	18.7	1.9
C_{R3}	10.21	2.71	1.26	7.34	1.90	4.44	4.86
C_{R1}/C_S	0.81	0.97	0.82	0.9	0.82	0.84	0.9
C_{e1}/C_{e2}	2.16	0.83	0.14	0.02	0.16	0.85	0.04
$C_{e1}+ C_{e2}$	47.84	47.99	39.52	49.36	39.96	43.66	25.85

GENERALIZED PARAMETERS

For the model to be useful in predicting the thermal loads and temperatures of rooms with displacement ventilation and chilled ceilings under a variety of conditions, it is clearly necessary to be able to generalize the parameters of the model. This requires the definition of functions or rules that could be used to establish the model parameters from either other model inputs or more conventional design parameters. The convection coefficient parameters are considered first.

The Convection Coefficient Parameters

It was necessary, as noted previously, to allow a different value of convection coefficient for the lowest section of the room walls than for the rest of the walls when calculating the parameters. There is some physical basis for making such a distinction between the lowest part of the walls and the upper part. Flow visualization and CFD results showed that, in the bottom part of the room, the flow is dominated by a gravity current from the diffuser and a return current flowing over it. In the upper part of the room, the flow is much more mixed, with higher velocities near the walls. The convection coefficients in the upper part of the room can therefore be expected to be larger.

In the calculations of the parameters, in nearly all the test cases, a value for the convection coefficient for the lower part of the walls that satisfies the constraints of the model could be found using the correlation published by Hatton and Awbi (1998) for turbulent flows in enclosures, i.e. $h_c=1.49(\Delta T)^{0.345}$ W/m^2.K. This then, seems a reasonable basis for defining the value of the parameter h_{wl} in the model.

It is more difficult to find independent correlations for convection coefficients representative of conditions at the ceiling. The value of the convection coefficient could be expected to lie between 4.3 W/m^2.K, which is the value given in the CIBSE Design Guide A for horizontal surfaces and still air conditions, and 24-96 W/m^2.K, which is the range of values for a plate with an impinging jet with similar characteristics to that of the plume (Gardon and Akfirat 1965). CFD results (Rees 1998) suggest values of h_c in the range 12.8-19.1 W/m^2.K.

The values of h_c found from the parameter calculations are higher for the cases without a chilled ceiling, 11.7 W/m^2.K, than for the cases with a chilled ceiling, 5.9 W/m^2.K.. There is also greater variation about the mean value of h_c in the displacement ventilation cases. The coefficient is less well defined in these cases than in the chilled ceiling cases because of the small temperature differences at the ceiling, and corresponding greater significance of the measurement errors. In view of the lack of good independent information concerning the value of the ceiling convection coefficient, the mean value found from the chilled ceiling test case parameter calculations has been adopted as a constant coefficient in the model.

The value of the floor heat transfer coefficient found in the parameter calculations is given by a single equation $h_f=C_s(T_{fla}-T_s)/(T_{fla}-T_{fl})A_f$. This equation can be solved independently of the others, given a value for T_{fla}. Nearly all the values calculated in this way fall in the range 1-3 W/m^2.K. Again, in the absence of better information, the mean value of the floor convection coefficient, 2.1 W/m^2.K, has been adopted to define a constant value of h_f in the model.

The Capacity Rate Parameters

In the process of considering trends in the model parameters, alternative methods of parameterizing the model were considered. The four independent capacity rate parameters were chosen initially to be the capacity rates representing flow into the plume(s), namely C_{fp}, C_{e1}, C_{e2} and C_{e3}. This method of parameterizing the model has the advantage that the parameters can be thought of a representing the entrainment processes and are always in the same direction, but has the disadvantage that the parameters are dimensionalized.

A similar method might be to specify the capacity rates between the room air nodes, namely C_{R1}, C_{R2}, C_{R3} and C_{R4}. These parameters have the disadvantage that they represent flows that are not always in the same direction in each form of the model. A further set of parameters could be defined by considering the ratio of flows where the flow divides in the network, such as C_{fp}/C_S. Each of these parameterizations was used, and the values for each case examined, in order to identify trends that could be used to form rules for determining parameter values.

Considering each of the sets of capacity rate parameters, it is apparent that some of the parameters do not show any particular variations with the usual design parameters such as load size, air change rate, or ceiling temperature. Some of the parameters vary but have values confined within definite limits. The trends in the capacity rate parameters can be summarized as follows (see Tables 1-3).

1. C_{fp}/C_S falls in the range 0.03-0.29 i.e. C_{fp} is always a limited fraction of the supply capacity rate.
2. Parameter C_{R3} falls within a relatively narrow range of 0.48-10.2 W/K and is always of similar magnitude to parameter C_{fp}.
3. The sum of parameters C_{e1} and C_{e2} is always very close to the supply capacity rate, C_S.
4. Parameter C_{e3}, which represents the entrainment at the top of the plume and degree of mixing in the upper part of the room, is relatively small in the displacement ventilation cases. It becomes large (up to 6.5 times the supply capacity rate) when the loads are large and/or the ceiling temperature is lower.

The small value of the parameter C_{fp} and the nearly constant value of C_{e1+} C_{e2} could be expected. The effect of these parameters is mainly to control the temperature gradient in the lower part of the room. The experimental results showed that the non-dimensionalized temperature gradients in the lower part of the room are very similar for test cases with the same supply capacity rate. The temperature gradients found in the experiments fall, therefore, into a relatively narrow range. Hence, the parameters controlling the prediction of the temperature gradient in the lower part of the room might be expected to fall into a limited range.

From these observations of the parameter variations, some rules can be defined that allow the approximate determination of the parameter values. Firstly, as C_{fp} varies little, its value can be set from the mean value of C_{fp}/C_S, i.e. 0.15. It also seems reasonable to set $C_{e1} + C_{e2} = C_S$. If this is done, continuity restraints dictate that $C_{R3} = C_{fp}$. Having established these rules it remains necessary to find the ratio C_{e1}/C_{e2} and the value of C_{e3}. The only notable trend concerning the value of C_{e3} is that for nearly all the displacement ventilation test cases its value lies towards the bottom of its range, such that $C_{e3}/C_S \approx 0.15$. For the displacement ventilation and chilled ceiling test cases, there is a much wider variation of C_{e3}.

The significance of the parameters C_{e1}/C_{e2} and C_{e3} was investigated by examining the model output using a wide range of values for these parameters. Varying C_{e3} chiefly varies temperature TR3 but has negligible effect on the overall air heat balance. The parameter ratio C_{e1}/C_{e2} influences T_{R2} and therefore the temperature gradient in the lower quarter of the room. Unfortunately, the data collected and the parameter values calculated do not show how the parameter ratio C_{e1}/C_{e2} can be readily established. For the purposes of testing the model further, and demonstrating how it could be used, this ratio has been set at 1.0. A summary of the rules that can be used to establish each of the model parameter values is shown in Table 4.

TESTING THE MODEL

The model was tested in the following ways,

- by making comparisons between the measured and predicted air heat balances;
- by making comparisons between the measured and predicted temperatures in the occupied zone.

If these calculations are made by fixing the inside surface temperatures at their experimental values and using the parameter values calculated for that particular case, the results are very nearly exact. In the tests reported below, however, the predictions have been made using the generalized parameter values defined by the rules given in Table 4.

The surface temperatures have been fixed at their experimental values in these tests. This was done in order to test the adequacy of the air flow network and associated parameters in the model. External boundary conditions could have been applied by extending the model with wall conductances, but modeling wall conduction is strictly beyond the scope of the model and would introduce additional uncertainties. The

room air heat balances and air temperatures (at node R2), for a selection of cases, are given in Table 5.

Table 4: Rules found for determining the model parameter values.

Parameter	Rule to set Parameter Value
h_f	2.1 W/m^2.K (mean calculated value)
h_c	5.9 W/m^2.K (mean calculated value)
h_w	3.0 W/m^2.K (CIBSE Guide A)
h_{wl}	$1.49(\Delta T)^{0.345}$ (Hatton and Awbi 1998)
C_{fp}	0.15 C_S
C_{e1}, C_{e2}	$C_{e1}+C_{e2}=C_S$ and $C_{e1}/C_{e2}=1$
C_{e3}	0.15 C_S for displacement ventilation, > 0.15 C_S for high loads and chilled ceiling cases

Table 5: Comparison of measured room temperatures and air heat balances (Q_a) with predicted values.

Test Case	Measured Q_a (W)	Predicted Q_a (W)	Measured T_{R2} (^{o}C)	Predicted T_{R2} (^{o}C)
DV8	58.5	74.5	22.10	22.12
DV12	212.8	235.8	21.37	21.48
DC10	248.9	209.8	24.33	23.68
DC11	164.7	162.8	21.85	21.98
DC14	162.4	157.9	18.28	18.53
DC15	242.2	239.3	19.08	19.11

The predicted value of the net load on the air stream, Q_a, is worst in case DC10, where the generalized parameter values are most different from the values specifically calculated for that test case. It is also in case DC10 that the load on the air stream is the smallest proportion of the total internal load (1200W).

Comparison of the measured room air temperature profiles with those calculated using the generalized parameters for displacement ventilation cases DV8 and DV12 is shown in Figure 7. Similar comparisons for displacement ventilation and chilled ceiling cases DC11 and DC15 are shown in Figure 8. The temperature profiles are reasonably well matched over the full height of the room.

To test the ability of the model to reproduce some of the characteristics of displacement ventilation and chilled ceiling systems further, a hypothetical test zone has been used. This zone was of the same geometry as the Loughborough test chamber but all the walls were given conductance of 0.3 W/m^2.K. A base test case was devised in which the outside temperatures were 25^{o}C, the ceiling temperature was 20 ^{o}C, the air supply temperature was 19^{o}C and flow rate equivalent to 3.0 air changes per hour. The load was set at 600W for the base case.

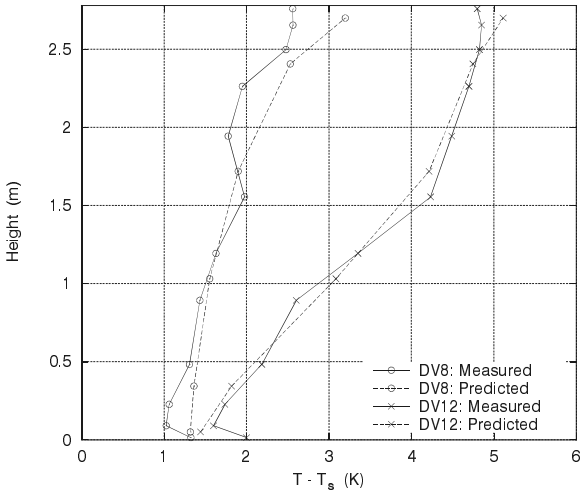

Figure 7: Comparison of Predicted and measured air and temperatures profiles for displacement ventilation cases DV8 and DV12.

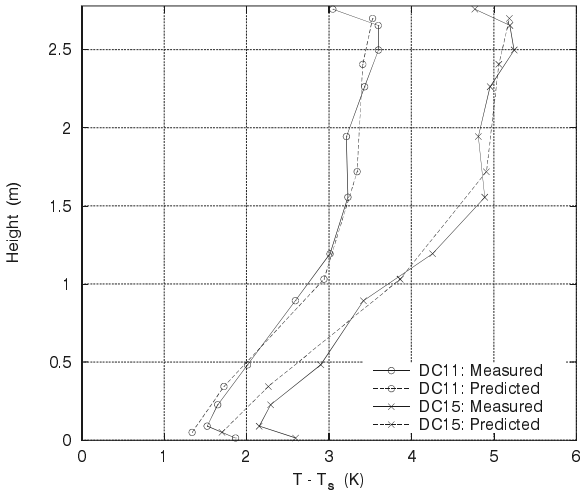

Figure 8: Comparison of Predicted and measured air and temperatures profiles for displacement ventilation & chilled ceiling cases DC11 and DC15.

The response of the model to changes in ceiling and air temperature is shown in Figure 9. The model can be seen to demonstrate the expected qualitative behavior, in that:

- as the supply air temperature is increased and approaches the external temperature the heat transferred to the air stream reduces;
- as the ceiling temperature is reduced, so the proportion of the load transferred to the air stream reduces and the comfort temperature becomes closer to the supply air temperature.

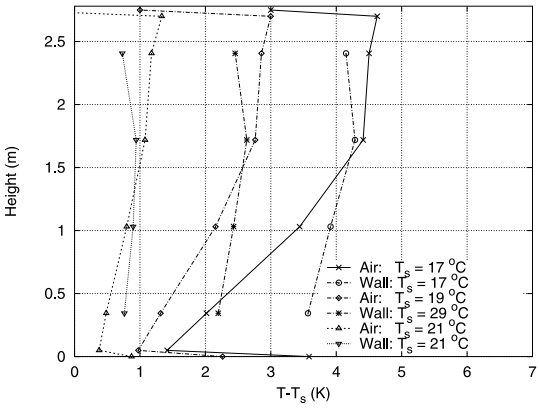

(i)

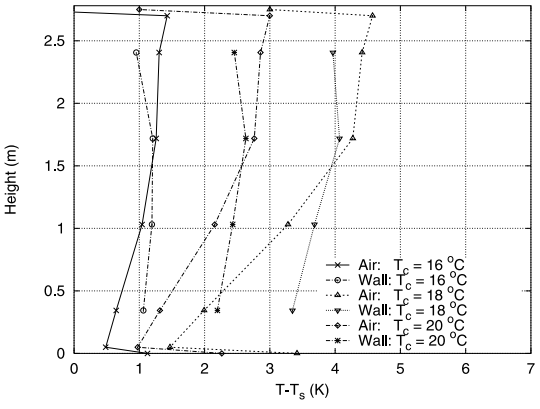

(ii)

Figure 9: Predicted air and wall surface temperatures from the model with (i) varying supply air temperature and (ii) varying ceiling temperature.

CONCLUSIONS

A nodal model has been developed to represent room heat transfer in displacement ventilation and chilled ceiling systems. The structure of the model includes air nodes representing different regions of the room air and air flowing in the plume(s). This structure allows the air and surface temperature gradients to be calculated. By separately representing the air movement in the plume(s) and the rest of the room, the model is able to correctly represent the relationship between the internal load and the air and surface temperatures found in the occupied part of the room.

A method has been demonstrated whereby capacity rate parameter values can be calculated by solving the heat and mass balance equations of the nodal model using the experimental temperatures as inputs. Convection coefficient parameters for the model have been defined using a combination of published correlations and calculated parameter values. Analysis of the calculated capacity rate parameters has produced a set of rules that enable the parameter values to be pre-determined. The model has been shown to be able to reproduce the measured air heat balance and room temperatures reasonably well. The ability to show the expected response to changes in the design parameters has also been demonstrated.

ACKNOWLEDGEMENTS

This work was funded jointly by British Gas plc, EA Technology, the Ove Arup Partnership and Loughborough University. The authors would also like to thank Y. Li for provision of experimental data and E.F. Sowell for his support in using the LIGHTS program.

REFERENCES

Awbi, H.B., Calculation of convective heat transfer coefficients of room surfaces for natural convection. Energy and Buildings, 28(2): 219-227, 1998.

CIBSE., CIBSE Design Guide Volume A, The Chartered Institute of Building Services Engineers, London, 1986.

Dalicieux, P. and Bouia, H. Présentation d'une méelisation simplifiée des mouvements d'air à l'intèrieur d'une pièce d'habitation. Electricite de France report HE 12 W 3269, pp. 29, 1993.

Gardon, R. and Akfirat, J., The role of turbulence in determining the heat transfer characteristics of impinging jets., International Journal of Heat and Mass Transfer 8: 1261-1272, 1965.

Hensen, J. and Huygen, B., Energy simulation of displacement ventilation in offices, Proc. of CIBSE National Conference, pp. 1-8, 1996.

Klien, S. and Alvarado, F., EES Engineering Equation Solver: User Guide, F-Chart Software, Wisconsin, 1997.

Li, Y., Sandberg, M. and Fuchs, L., Vertical temperature profiles in rooms ventilated by displacement: Full-scale measurement and nodal modeling, Indoor Air (2): 225-243, 1993.

Mundt, E., The performance of displacement ventilation systems-experimental and theoretical studies, PhD thesis, Royal Institute of Technology, Stockholm, 1996.

Rees, S. J. and Haves, P., A Model of a Displacement Ventilation System Suitable for System Simulation, Proc. of 'Building Simulation-95', Madison, Wisconsin, August 14-18. 1:199-205. 1995.

Rees, S. J., Modeling of Displacement Ventilation and Chilled Ceiling Systems using Nodal Models. Ph.D. Thesis, Loughborough University. 1998.

Sowell, E. F., LIGHTS User's Guide, Department of Computer Science, California State University. CA, USA, 1989.